



**Ultrahigh Sensitivity Wearable Sensors Enabled by
Electrophoretic Deposition of Carbon Nanostructured
Composites onto Everyday Fabrics**

Journal:	<i>Journal of Materials Chemistry C</i>
Manuscript ID	TC-COM-10-2021-005132.R1
Article Type:	Communication
Date Submitted by the Author:	15-Dec-2021
Complete List of Authors:	Doshi, Sagar ; University of Delaware Murray, Colleen; University of Delaware, Department of Materials Science and Engineering Chaudhari, Amit; University of Delaware, Department of Mechanical Engineering Sung, Dae Han; University of Delaware, Department of Mechanical Engineering Thostenson, Erik; University of Delaware, Department of Mechanical Engineering

Ultrahigh Sensitivity Wearable Sensors Enabled by Electrophoretic Deposition of Carbon Nanostructured Composites onto Everyday Fabrics

Sagar M. Doshi^{a,b}, Colleen Murray^{a,c}, Amit Chaudhari^{a,b},
Dae Han Sung^{a,b}, Erik T. Thostenson^{a,b,c,*}

a – Department of Mechanical Engineering, University of Delaware, Newark, USA

b – Center for Composite Materials, University of Delaware, Newark, USA

c – Department of Materials Science and Engineering, University of Delaware, Newark, USA

* – Corresponding author – thosten@udel.edu

ABSTRACT

Wearable sensors are of increasing interest in emerging applications such as human-computer interaction, electronic skin, smart robotics, and rehabilitation monitoring. Here we report a novel garment-based sensor by integrating nanocomposite coatings on commercially available fabrics. The sensing fabric is soft to the touch, breathable, and shows ultrahigh sensitivity of the electrical response to fabric deformation. A water-based electrophoretic deposition (EPD) technique at room temperature is used to deposit the nanocomposite films of polyethyleneimine (PEI) functionalized carbon nanotubes (CNT). The thin film nanocomposite creates an electrically conductive piezoresistive sensing network by uniformly coating the individual fibers within the fabric, and the coating is chemically bonded to the fiber surfaces. When integrated into garments, the sensors show remarkable sensitivity (~3000% resistance change) to elbow/knee motion. In addition to large joint motion, the sensors are able to detect delicate motions, such as finger movement and muscle contraction. We demonstrate the ability to deposit CNT-PEI nanocomposite coatings on commercially available fabrics with different textile structures and natural/synthetic fibers such as wool,

rayon, polyester, cotton and nylon. The industrial scalability of the EPD process, combined with the resulting textile sensors' extraordinary sensitivity, offers the potential to develop the next generation of wearable functional garments.

Keywords: wearable technology; carbon nanotubes; smart fabrics; piezoresistive sensors; human motion analysis

With the emergence of the 'Internet of Things' and the ability to analyze large amounts of data, considerable attention has been given to the development of wearable technology. While most commercial applications focus on the detection of vital signs or activity levels, there is an increasing focus on lightweight and flexible sensors that are capable of capturing physiological and biomechanically-relevant information. Sensors that can be seamlessly incorporated into clothing have a wide range of potential applications, including virtual health and rehabilitation, athletics performance monitoring, soft robotics, and augmented/virtual reality. ^[1,2] Critical attributes required for materials used in such wearable sensors include the sensitivity to motion detection as well as low power requirements, stretchability/flexibility, durability, and wearing comfort.

Owing to the potential for integration of strain-sensitive materials into clothing, a wide range of different approaches have been reported. Many sensors, such as traditional metallic materials for strain sensing, are rigid and have limited flexibility. This affects both the ability of the sensor to detect large deformations and can make the sensor intrusive and uncomfortable to wear. In recent years, nanostructured materials and composites have offered potential as emerging strain sensors, and capacitive and piezoresistive flexible sensors have been developed using a variety of different nanomaterials and novel micro/nano structures. Unlike a typical metallic strain gauge, where the measured electrical resistance is altered largely due to dimensional changes (axial strain and Poisson contraction), the electrical resistance change of many nanostructured sensors results from local electrical contacts, either through nanoscale electrical tunneling between particles or micro/meso scale re-arrangement of structures. Carbon nanotubes are often utilized as nanoscale reinforcements due to their large aspect ratio (length/diameter) and electrical conductivity. The large aspect ratio reinforcement enables the creation of electrically conductive networks that establish a nerve-like mechanical/electrical sensing response due to the strain-induced CNT-CNT electrical tunneling resistance.

Among the most common approaches for creating flexible strain sensors is the direct mixing of electrically conductive materials with elastomeric polymers, such as polydimethylsiloxane (PDMS). Commonly used conductive fillers include carbon black, graphene, carbon nanotubes and metal nanoparticles. [3-11] While this technique is popular because of the relative ease of manufacturing by dispersing the conductive material in the bulk elastomer, one of the drawbacks of these nanocomposite sensors is that the sensor, itself, is not breathable. Also, the addition of high Young's modulus reinforcements to the elastomer can drastically increase the elastomer stiffness. The lack of breathability and the stiffening of the sensor can affect the comfort of wearing. Integration of the nanoscale reinforcement, in addition to elastomer aging and water absorption, can also make these types of sensors brittle.

Some of the other techniques used by researchers include the use of conductive polymers such as poly(3,4-ethylenedioxythiophene) PEDOT, [12,13] polypyrrole (PPy) [14,15] and polyaniline (PANI). [16,17] Due to their excellent stretchability, the use of hydrogels [18-20] has also been investigated to create flexible sensors. Flexible sensors based on piezoelectric [21-23] and triboelectric [24-27] mechanisms have also been explored, which may offer the additional advantage of simultaneously harvesting energy. Despite the tremendous potential and benefits of these sensors, key challenges in scalability, user comfort, and non-invasive integration with commercially used fabrics remain an ongoing barrier that needs to be overcome.

Therefore, fabric based wearable sensors, where the sensor is integrated directly into the textile structure, are promising candidates due to their potential ease of integration in garments and increased comfort of use. The intermeshed, intertwined structure of the fabrics makes them a suitable candidate for wearable sensors, which can provide repeatable and reliable sensing response.

To create fabric-based conductive sensors, carbon-rich materials may be carbonized through thermal decomposition. For example, carbonization of cotton and silk-based fabrics have been utilized for making fabric-based sensors. [28,29] Pyrolysis processes can be

extremely energy intensive and are limited to a relatively small range of materials. In addition to these challenges, the resulting materials are often stiff and brittle. Other approaches have examined the use of creating conductive yarns by either co-mingling with metallic fibers or plating metals onto fibers.^[30–32] For coated fibers, poor adhesion of metallic coatings, increased stiffness and a change in fabric texture are key drawbacks of these approaches. Key challenges associated with the large-scale applications of these wearable sensors include complex manufacturing, compatibility with existing production techniques in the textile industry, and non-invasive integration into commonly worn garments. Therefore, there exists a critical need for developing flexible wearable sensors that can be manufactured and integrated with relative ease with existing textile infrastructure and are cost-effective, stretchable, and are comfortable to wear for the end user.

Here we demonstrate a new wearable garment-based sensor with extraordinary sensitivity. The sensor is enabled by an efficient electrophoretic deposition (EPD) process where multi-walled carbon nanotubes functionalized with polyethyleneimine (CNT-PEI) create a thin nanocomposite coating, < 500 nm, on the surfaces of individual fibers throughout the fabric.^[33–35] EPD is performed from an aqueous dispersion at ambient temperatures under a direct current (DC) electric field. The coating process is rapid, repeatable, and environmentally benign. Only a fraction of a gram of functionalized CNTs, which cost ~\$1.5/gram, are deposited. EPD is also industrially scalable as a roll-to-roll process where the potential exists to produce large quantities of sensor fabric. Due to the nature of the coating, there is no significant change in the texture and the feel of the fabric, and the fabric porosity is also maintained, making it comfortable to wear. The CNT-PEI nanocomposite coating adds negligible mass to the fabric, is robustly bonded to the fibers, and does not deteriorate when subjected to durability tests. Upon integration into garments, the sensor displays extremely high sensitivity with a resistance change in the range of 3,000 % when worn on the elbow/knee during flexion-extension. The high sensitivity also enables the detection of minute

finger motion during writing with a pen and minuscule movements due to muscle contractions.

The EPD process is a highly efficient and scalable technique to create uniform films of functionalized nanostructures onto fibers, and the driving mechanism is the mobility of the functionalized nanoparticles under an applied electric field followed by growth of the film as an extension of the electrode. ^[36,37] Figure 1a shows a schematic of the functionalization and deposition process for multi-walled carbon nanotubes where the nanotubes are dispersed in water and oxidized using ozone gas, followed by grafting of branched PEI. The PEI protonates under acidic conditions and results in a positive charge. The positively charged CNT-PEI repel each other to create a stable dispersion in water and enable deposition at the cathode under applied fields. The non-conductive fabric to be coated is placed in direct contact with the cathode, as shown in Figure 1c. When a DC electric field is applied, a uniform CNT-PEI nanocomposite coating is created on all fibers throughout the fabric, not just the fibers at the surface. The deposition process is not a direct line of sight mechanical deposition but initiates at the electrode and extends onto the fibers in direct contact with the electrode. The deposited carbon nanotube nanotubes are electrically conductive and hence act as an extension of the electrode advancing the deposition through the fiber bundles through the thickness of the fabric. ^[34] Sung et al. ^[34] show that it is possible to deposit nanocomposite coating in a pattern by using patterned electrodes. This is a potential route to improve sensitivity in future research by depositing nanocomposite coatings in specific patterns.

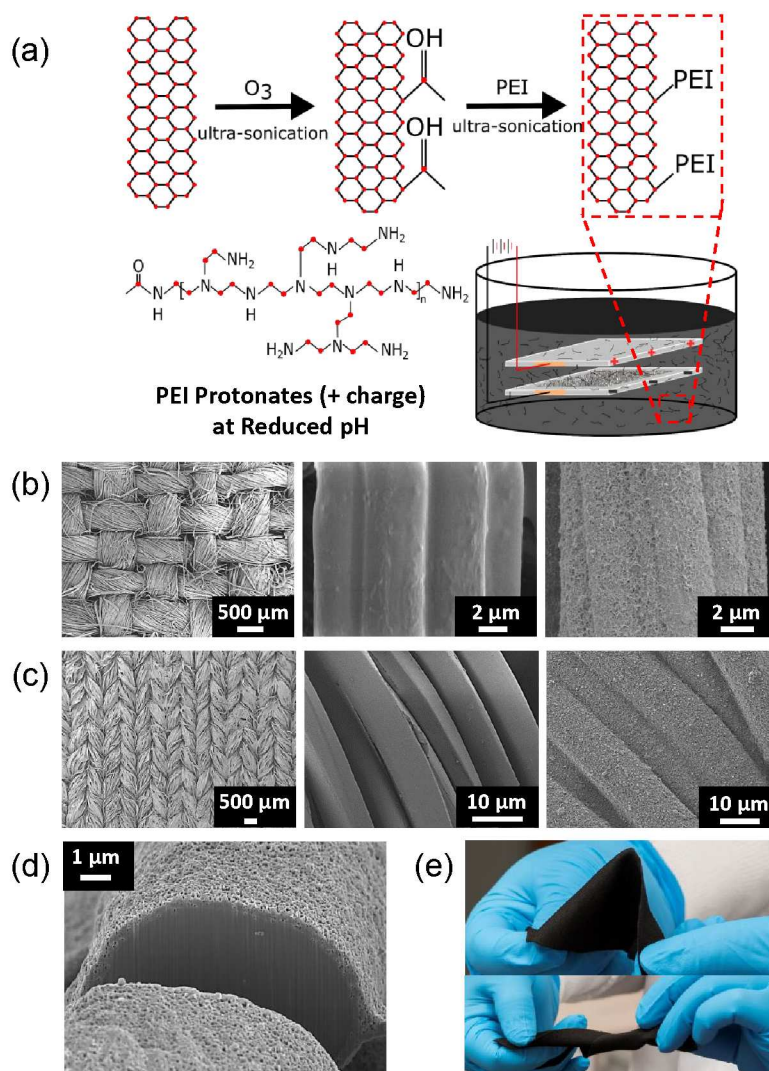


Figure 1. (a) Processing of CNTs using continuous ultrasonication and functionalization with ozone followed by PEI, the chemical structure of PEI with amine groups, which protonate under mildly acidic conditions, and a schematic diagram of EPD in an aqueous bath where the fabric is in contact with the cathode; (b) from left: plain woven rayon fabric, uncoated fiber showing longitudinal striations, and CNT-PEI coated rayon fiber, (c) from left - knitted fabric with co-mingled fibers (polyester, nylon and elastane), uncoated fiber bundles, and bundles uniformly coated with CNT-PEI, (d) a cross-section of fiber in (c) showing the porous CNT-PEI coating with a constant thickness around the fiber and (e) photographs of the fabric in (c) with high flexibility and stretchability after CNT-PEI coating.

A critical advantage of this EPD process is the ability to coat various natural and synthetic fibers such as rayon, cotton, polyester, nylon and wool (see supporting information, Figure S1). Using the same setup, carbon nanotubes were deposited on these different fabrics with varying material composition, weaving patterns and microstructures. Figures 1b and 1c are a series of scanning electron microscope (SEM) images showing the textile structure, fiber-level texture, and the morphology of the CNT-PEI coating. Figure 1b is a plain-woven fabric of rayon fibers, while Figure 1c is a knitted fabric consisting of polyester, nylon and elastane fibers. The SEM image of the uncoated rayon fiber shows a distinctive surface texture with linear striations along the fiber length, and this surface texture is also visible after applying the CNT-PEI coating. Despite the different textile structures and fiber types, all the fibers within the fabric are uniformly coated. Figure 1d shows a cross-section of a single fiber where a focused ion beam was used to cut the fiber and observe the structure and uniformity of the coating. The CNT-PEI deposited onto the fiber creates a porous nanocomposite coating with a uniform thickness that completely surrounds the fiber. The coating layer is extremely thin, on the order of a few hundred nanometers, and there is no significant change in the fabric stiffness and is soft to the touch. Figure 1e shows the stretchability and the flexibility of the CNT-PEI coated fabric.

Our prior research has established that CNT-PEI films are piezoresistive, where strain results in a measurable change in the nanocomposite electrical resistivity. With the goal of creating fabric-based wearable sensors for monitoring human motion, we performed electromechanical characterization on a variety of different fibers and fabric types. From this initial characterization, we down-selected fabric for more detailed characterization and integration into compression sleeves to monitor joint motion. The fabric selected is a commercially available knit fabric consisting of polyester, nylon and elastane (Figure 1c). **Figure 2a** shows the electrical-mechanical response when the fabric is strained in tension along the wale direction (in the direction of the loops). The resistance change is reported as a

normalized resistance change to reduce the effect of the baseline dimensions of the sensor. The fabric shows a nonlinear response that is likely due to different electrical conduction mechanisms at length scales ranging from the fiber-level to macro-scale deformation of the fabric structure. At the fiber level, strain in the fiber gives rise to changes in electrical tunneling in the CNT-PEI film and the nanocomposite piezoresistive response. Within the fiber bundle, transverse compaction under tension brings the fibers in the bundle into contact, and at the fabric level, the loops of the knit change shape. At strains below 3%, the fabric shows a bi-linear resistance-strain response. At low strain, below 0.8%, the response is linear and shows a gauge factor (fractional resistance change/strain) of approximately 125. Above 0.8% strain, there is a sharp increase in the slope where the calculated gauge factor increases significantly to about 350. In comparison, a traditional metallic strain gauge has a gauge factor of approximately 2. Near the transition region, there is a clear change in the structure of the knitted fabric. Upon stretching, the curved part (the loop's head) becomes narrower, and the length of the loop's leg becomes more extended, making each column of the loop narrower. As a result, the loops likely break contact with loops in the adjacent column, creating a larger change in the electrical resistance. At higher strains, the sensing response becomes nonlinear and plateaus at strains above 5% with a total resistance change of the sensor above 1200%. At higher strains, there is a clear Poisson's effect in the fabric, where the transverse contraction under strain is significant. There was a significant difference in the fabric structure located near the grips, where the fabric is constrained in the transverse direction, and the center of the fabric specimen. If worn in a compression garment to measure body motion, the transverse deformation of the fabric will be uniformly constrained.

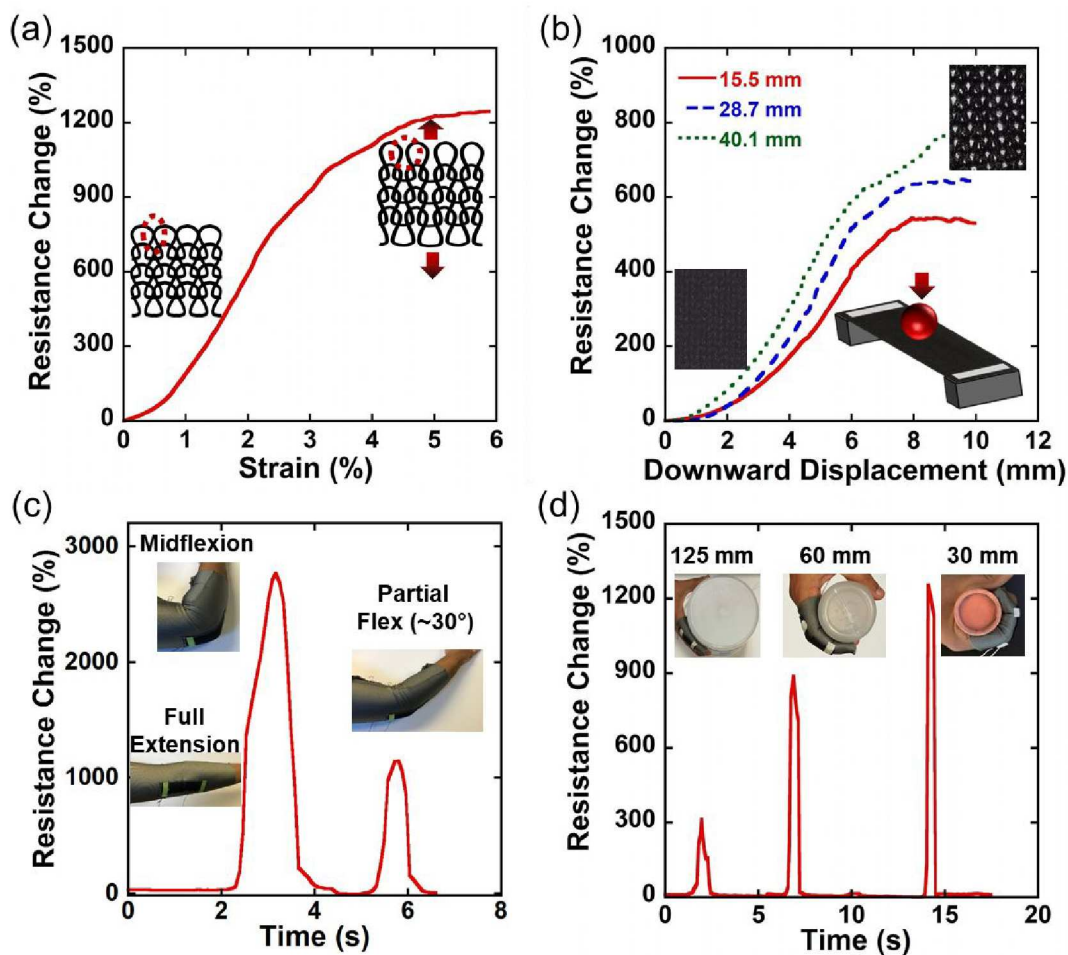


Figure 2. (a) Electrical response of the sensor under uniaxial tension, (b) sensor response under spherical indentation (biaxial stretching), (c) sensor integrated into a compression sleeve showing extraordinarily high sensitivity, with a resistance change of $\sim 2750\%$ at midflexion of the elbow and (d) ability of the sensor to detect delicate finger bending movements, resistance change is proportional to the bending of finger.

In order to examine the influence of biaxial stretching on the fabric electrical response, non-conductive spheres of varying diameter were pushed into the fabric that was fixed to a support. **Figure 2b** shows the mechanical-electrical response. The fabric is stretched biaxially, along the length and the width, due to the spherical shape, and larger diameter spheres result in more biaxial stretching. Inset to the graph shows photographs of the fabric deformation, where under no strain, the knitted fabric shows a tightly interlaced structure

while the structure under biaxial stretching shows the opening of the looped knit structure. The larger diameters result in a higher electrical resistance response. Similar to the axial resistance response, the change in electrical resistance plateaus at higher deformations, but the increased bi-axial stretching of the 40 mm sphere keeps the sensor from plateauing completely at a downward displacement of 10 mm.

Figure 2c shows the sensing response when the sensor is integrated into an elbow sleeve having a compression fit to avoid slipping during movements. After wearing the compression sleeve onto the arm with the sensor positioned over the elbow joint, the initial resistance in the unstretched state is recorded with the arm fully extended. When the elbow is flexed, there is an extremely large change in the sensor electrical resistance. At a partial flex of $\sim 30^\circ$, a resistance change of 1250% and at midflexion ($\sim 90^\circ$), a remarkable 2750% resistance change is observed. Much like testing of the fabric with different diameter spheres, the sleeve is stretched in both axial and transverse directions along the arm's length. This causes a very high change in electrical resistance, which is directly proportional to the angle at the elbow (see supplemental material, video V1). The change in sensor electrical resistance is significantly greater for these tests than the axial stretching in Figure 2a, likely because of the biaxial stretching over a large area. The limit of detection for uniaxial strain is about 5%, but for human movements at joints, the entire range of motion can be measured. In terms of traditional definition of sensitivity using gauge factors, there are multiple studies that have reported higher sensitivity measured using typical uniaxial tests. ^[38,39] However, in response to human joint movement, our sensors display extremely high sensitivity. With the remarkable sensitivity to arm motion, similar finger sleeves were fabricated to examine the ability of the sensors to detect the more delicate finger motion. **Figure 2d** shows the sensor response due to gripping items of varying diameter, where smaller diameter objects result in higher finger curvature and hence a greater change in electrical resistance. For the smallest diameter of 30 mm, the sensor electrical resistance change is over 1200%. The ability to

detect large motion at the elbow and small finger movements with extremely high sensitivity enable applications in human motion analysis such as monitoring the range of motion of the arm at the elbow joint during a rehabilitation process.

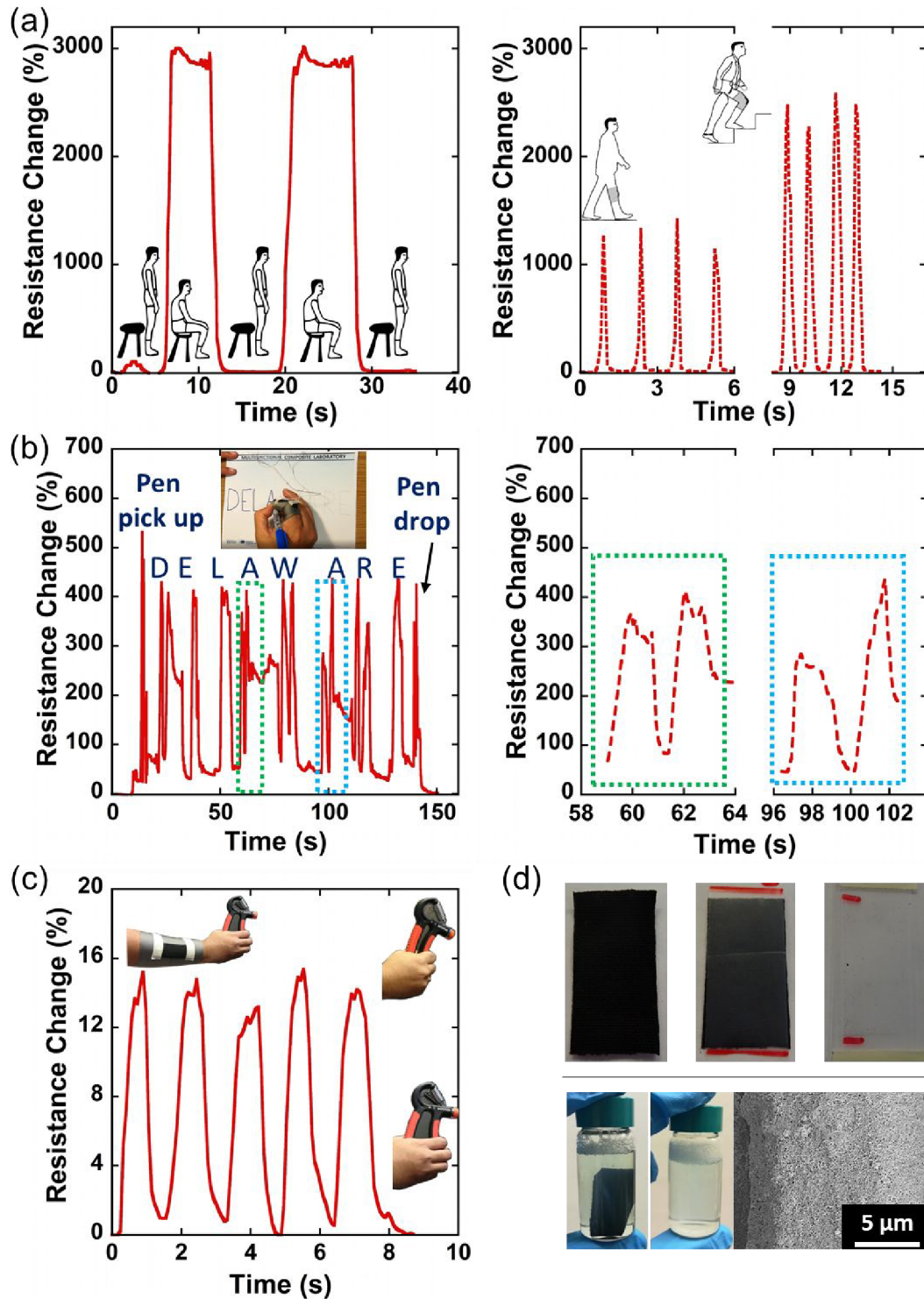


Figure 3. (a) Sensor integrated into a knee-sleeve displaying remarkable sensitivity due to knee bending in (left) sit-stand positions and (right) walking on flat ground and walking up the stairs, (b) finger sensor on the index finger showing (left) the word 'DELAWARE' being written and (right) similar response for writing the letter 'A,' (c) sensor worn over the forearm showing the ability to detect extremely small muscle contraction using a hand grip, and (d) durability of the fabric (top, from left) tape lift-off test showing the fabric, fabric with bonded tape, and tape removal and (bottom, from left) sonication showing fabric in water with detergent, clarity of water after sonication indicating that there was negligible damage or removal of the coating, and SEM micrographs showing the coating after sonication.

Additional experiments were conducted to examine the efficacy of these sensors for different applications. There is broad interest in utilizing sensors to monitor human gait outside of a laboratory setting and to quantitatively monitor the range of motion.^[40] This is specifically useful for patient rehabilitation after injuries or joint replacement surgeries. Gait analysis is traditionally done in a laboratory setting using motion capture cameras, which is expensive and time-consuming. Additionally, the subject can only be monitored for a limited amount of time in a controlled environment. Using wearable sensors that can be integrated into clothing enables human motion analysis for extended periods and outside of a laboratory setting -- in the patient's natural work or home environment. To examine the potential of these sensors to monitor human gait, a fabric sensor was integrated into a knee sleeve. The sensor was calibrated in the standing position to examine the capability of the sensor to capture knee motion with the subject sitting and standing, shown in **Figure 3a**. At ~3 seconds, when a small sudden movement is made, an increase in resistance is observed. When the subject sits on a chair, the knee is bent, causing a striking ~3000% resistance increase. As the person continues to sit, no significant change in resistance is observed. Upon standing, the resistance returns to its original value and stays constant until the next sitting motion. Figure 3a also shows the sensing response when walking on flat ground and walking up the stairs wearing

the knee sleeve with the carbon nanotube sensor integrated. When walking on flat ground, the knee is bent slightly during each step, causing an increase of about 1300% in electrical resistance. While walking up the stairs, the resistance change is almost 2500% for each step as each knee is bent more during the ascent.

The sensitivity to delicate finger motion (Figure 2d) offers potential for glove-based sensors that could be used for applications ranging from handwriting and sign language to human-computer interaction. **Figure 3b** shows the resistance response when a finger sleeve sensor is worn over the index finger, and the word 'DELAWARE' is written in capital letters (see supplemental material, video V2). The ultrahigh sensitivity of the carbon nanotube-based sensor can easily capture the small movements of the finger when writing. Even limited movements to pick up the marker from the table and keep it back after writing cause a resistance change of over 400%. The graph to the right in Figure 3b shows the sensing response for writing the letter 'A' in the word 'DELAWARE,' the 4th and the 6th letter. The resistance signature for both the letters 'A' are similar, where the peaks are due to the finger movements to draw the two angled lines. This enables potential applications in gesture recognition, where fingers are often used to make signs.

The sensor is so sensitive that it is also able to detect minuscule muscle contractions. Because of the ultrahigh sensitivity to delicate finger motion, additional experiments were performed to examine the capability to detect muscle contraction. **Figure 3c** shows the sleeve integrated with the sensor worn over the forearm while using a resistance exercise hand grip. When gripping the spring-activated device, the forearm flexors are activated, causing the muscles to expand, and stretching of the sensor—repeated gripping results in a repeatable change in electrical resistance. Video V3 in supplemental materials shows the sensor response when the fist is clenched and resulting in a change in the sensor's electrical resistance. The ability to detect muscle contractions enables promising applications in measuring muscle actuation in a non-invasive and comfortable manner.

In our prior research, we examined the deposition and adhesion of CNT-PEI films onto advanced fibers, such as carbon or glass.^[34] Detailed surface analysis shows that the CNT-PEI forms chemical bonds with the fiber surface in addition to forming chemical links within the deposited network of CNTs. Based on our success in depositing CNT-PEI onto a variety of different fibers lead us to hypothesize that the CNT-PEI also forms a bond with the surface of the fibers used in this work. Fibers and textiles often undergo surface treatments that likely create oxide groups on the surface of the fibers where the PEI can bond. Tape tests and sonication tests were conducted to examine the robustness of the carbon nanotube coating on the fibers. **Figure 3d** shows the steps in a tape test where a Scotch™ tape is bonded to the coated fabric and subsequently pulled off. After pulling the tape, some small fiber pieces and black residue was observed only along the specimen's edge. Under higher magnification it was revealed that fibers had broken and were pulled out of the fabric, likely due to the fiber ends cut using scissors. For the sonication tests, the fabric was placed in a glass vial containing tap water (Supporting Information, Figure S2) and tap water with detergent (Figure 3d) and sonicated in a bath sonicator for 15 minutes. Like the tape tests, there was no noticeable residue in the water after the tests indicating a robust bonding of the coating to the fibers. When viewed using an SEM after sonication, there was no visible damage to the CNT-PEI coating. When the fabric was weighed before and after the tape and sonication tests, there was no reduction in weight when measured using a weighing scale with the capacity of 0.0001 gram.

In conclusion, an ultra-high sensitivity, comfortable wearable sensor has been demonstrated by depositing thin and uniform nanostructured CNT-PEI films on various commonly used fibers and fabrics. The sensor displays remarkable sensitivity and the versatility to measure the human motion of different types. Since the CNT-PEI coating is an extremely thin layer, the flexibility and texture of the wearable sensor do not change significantly, making them comfortable to wear for the end-user. The CNT-PEI film is

robustly bonded on the surface of the fibers, as seen in the preliminary experiments conducted using tape tests and sonication. The sensing mechanism is investigated, and real-world applications are demonstrated. When integrated into sleeves worn over the knee/elbow to measure the range of motion, an exceptional $\sim 3000\%$ change in resistance is observed. Upon integration into finger sleeves, the sensor demonstrates the ability to measure extremely small finger movements due to writing. The sensor also establishes the capability to detect minute muscle contractions. These fabric-based, ultra-high sensitivity, comfortable-to-wear sensors have the potential to revolutionize and stimulate growth in wide-ranging potential applications from analyzing human gait and measuring range of motion in an affordable and out of laboratory setting to gesture recognitions and functional garments.

Experimental Section

Processing of carbon nanotubes to create aqueous dispersions: 2 grams of commercially available multi-walled carbon nanotubes CM – 95 (Hanwha Nanotech, South Korea) was weighed and mixed with 2 liters of ultrapure water (18.2 M Ω). Ultrasonication and ozonolysis technique described by An et al. ^[41] is used to create the aqueous dispersion of carbon nanotubes. After stirring for 15 minutes using a magnetic stirrer, the flask was then maintained at a temperature of 5°C using a cooling bath. A probe sonicator (Sonicator 3000, Misonix) was used with a duty cycle of 15 seconds on and 10 seconds off. A peristaltic pump was used for circulating the carbon nanotube dispersion through a continuous flow cell. While sonicating, ozone gas produced using an oxygen concentrator (OxyMax 8, Longevity Resources) and ozone generator (Ext 120-T, Longevity Resources) and bubbled into the dispersion at a rate of ~ 500 ml/min. After ozone functionalization, 2 grams of branched polyethyleneimine (PEI) was added, and the sonication is continued for another 4 hours. Glacial acetic acid was then added to decrease the pH to ~ 6 , which causes the protonation of the amine groups in PEI, imparting the charge to the nanotubes, enabling the creation of a stable dispersion as well as electrophoresis.

Sensor Fabrication: The fabric to be coated was backed against a stainless steel (316) electrode connected to the negative terminal because the carbon nanotubes are positively charged. Elastic bands are used for ensuring slight tension in the fabrics to maintain uniform contact with the electrode. The uniform contact is essential because the formation of gases due to electrolysis can create bubbles, leading to non-uniform deposition on the fabrics. A counter electrode, also fabricated from stainless steel, was placed parallel to the anode at a fixed distance using insulating spacers. The assembly was then placed in a glass container with the carbon nanotube dispersion. The electrophoretic deposition is conducted by applying a DC voltage. The specimens were coated using a DC-EPD process under a field strength of 28 V/cm for 16 minutes. The size of the tension specimens is 100 mm x 25 mm. Following the coating, the fabrics were dried in an oven at 120°C. The fabric used for mechanical characterization is a commercially available, weft-knitted fabric consisting of 44% nylon, 43% polyester and 13% elastane. The size of the sensor for axial tests is 100 mm x 25 mm, and the one integrated into a sleeve is 125 mm x 37.5 mm. After deposition of the carbon nanotube film, the sensor is pre-stretched to approximately 50% strain before characterization. The pre-stretching enables a more repeatable sensing response as the first stretch may cause the nanocomposite coating between some adjacent fibers to break and lead to a more stable nanocomposite coating. The sensor was sewn into a compression sleeve using a sewing machine (Husqvarna Emerald 116). A 'zig-zag' pattern was selected to allow for stretchability.

Electromechanical Characterization: After the coating, flash dry silver paint (SPI Supplies) and two-part conductive epoxy (Epoxyies etc.) were used to mark the electrodes and attach lead wires to reduce the contact resistance and measure the electrical resistance accurately. The mechanical tests were conducted using a screw-driven load frame, Instron 5567, under displacement-control. The electrical measurements were done with a two-wire technique using a Sourcemeter (Keithley 6430). A constant source voltage of 20 V was applied, and the current was measured to calculate the resistance values. The electrical and

mechanical readings were synchronized using LabView software. The durability tests were conducted using the Scotch Tape™ test with 25 mm wide tape stuck to the fabric and left on for 3 minutes before peeling it off. The sonication tests were conducted using a bath sonicator (Branson) in a vial containing tap water for 15 minutes with a commercial detergent.

Scanning Electron Microscopy: SEM images were captured using an Auriga 60 Crossbeam electron microscope with an accelerating voltage of 3 kV for the carbon nanotube coated specimens. The specimens were coated with a Pd/Au layer using a sputter coater to reduce the charging of the specimen. The cross-section of the fiber is cut using a focused ion beam (FIB). First, a rough cut is made, followed by a fine cut with a FIB probe setting of 30kV and 240pA.

Supporting Information

Supporting Information is available for this manuscript.

Acknowledgements

The authors acknowledge funding support from the National Science Foundation (Grant 1254540), the UNIDEL Foundation and the Delaware INBRE program with a grant from the National Institute of General Medical Sciences - NIGMS (P20 GM103446). Help from Cheyenne Smith and Dr. Huantian Cao from the Fashion and Apparel Science department at the University of Delaware for sewing techniques is appreciated. Dr. Zhao's support for focused ion beam and electron microscopy is appreciated.

References

- [1] W. A. D. M. Jayathilaka, K. Qi, Y. Qin, A. Chinnappan, W. Serrano-García, C. Baskar, H. Wang, J. He, S. Cui, S. W. Thomas, S. Ramakrishna, *Adv. Mater.* **2019**, *31*, 1.
- [2] A. Nag, S. C. Mukhopadhyay, J. Kosel, *IEEE Sens. J.* **2017**, *17*, 3949.
- [3] J. Shintake, E. Piskarev, S. H. Jeong, D. Floreano, *Adv. Mater. Technol.* **2018**, *3*, DOI 10.1002/admt.201700284.
- [4] J. Zhu, H. Wang, Y. Zhu, *J. Appl. Phys.* **2018**, *123*, 034505.
- [5] T. T. Tung, M. J. Nine, M. Krebsz, T. Pasinszki, C. J. Coghlan, D. N. H. Tran, D. Losic, *Adv. Funct. Mater.* **2017**, *1702891*, 1702891.
- [6] S. Lee, S. Shin, S. Lee, J. Seo, J. Lee, S. Son, H. J. Cho, H. Algadi, S. Al-Sayari, D. E. Kim, T. Lee, *Adv. Funct. Mater.* **2015**, *25*, 3114.
- [7] Z. Zou, C. Zhu, Y. Li, X. Lei, W. Zhang, J. Xiao, *Sci. Adv.* **2018**, *4*, eaaq0508.
- [8] N. N. Jason, S. J. Wang, S. Bhanushali, W. Cheng, *Nanoscale* **2016**, *8*, 16596.
- [9] S. M. Jung, D. J. Preston, H. Y. Jung, Z. Deng, E. N. Wang, J. Kong, *Adv. Mater.* **2016**, *28*, 1413.
- [10] T. Yamada, Y. Hayamizu, Y. Yamamoto, Y. Yomogida, A. Izadi-Najafabadi, D. N. Futaba, K. Hata, Y. Hayamizu, K. Hata, Y. Yamamoto, T. Yamada, A. Izadi-Najafabadi, Y. Yomogida, *Nat. Nanotechnol.* **2011**, *6*, 296.

- [11] J. Lee, S. Kim, J. Lee, D. Yang, B. C. Park, S. Ryu, I. Park, *Nanoscale* **2014**, *6*, 11932.
- [12] M. Z. Seyedin, J. M. Razal, P. C. Innis, G. G. Wallace, *Adv. Funct. Mater.* **2014**, *24*, 2957.
- [13] T. Bashir, M. Ali, N. K. Persson, S. K. Ramamoorthy, M. Skrifvars, *Text. Res. J.* **2014**, *84*, 323.
- [14] M. Li, H. Li, W. Zhong, Q. Zhao, D. Wang, *ACS Appl. Mater. Interfaces* **2014**, *6*, 1313.
- [15] Y. Li, X. Y. Cheng, M. Y. Leung, J. Tsang, X. M. Tao, M. C. W. Yuen, *Synth. Met.* **2005**, *155*, 89.
- [16] M. Tian, Y. Wang, L. Qu, S. Zhu, G. Han, X. Zhang, Q. Zhou, M. Du, S. Chi, *Synth. Met.* **2016**, *219*, 11.
- [17] N. Muthukumar, G. Thilagavathi, T. Kannaian, *High Perform. Polym.* **2015**, *27*, 105.
- [18] Y. J. Liu, W. T. Cao, M. G. Ma, P. Wan, *ACS Appl. Mater. Interfaces* **2017**, *9*, 25559.
- [19] S. Xia, S. Song, G. Gao, *Chem. Eng. J.* **2018**, *354*, 817.
- [20] Y. Li, X. Xiong, X. Yu, X. Sun, J. Yang, L. Zhu, G. Qin, Y. Dai, Q. Chen, *Polym. Test.* **2019**, *75*, 38.
- [21] X. Ren, Y. Dzenis, in *Mater. Res. Soc. Symp. Proc.*, Cambridge University Press, **2006**, pp. 55–61.
- [22] N. R. Alluri, S. Selvarajan, A. Chandrasekhar, B. Saravanakumar, J. H. Jeong, S. J. Kim, *Compos. Sci. Technol.* **2017**, *142*, 65.
- [23] J. Zhu, L. Jia, R. Huang, *J. Mater. Sci. Mater. Electron.* **2017**, *28*, 12080.
- [24] F. Yi, L. Lin, S. Niu, P. K. Yang, Z. Wang, J. Chen, Y. Zhou, Y. Zi, J. Wang, Q. Liao, Y. Zhang, Z. L. Wang, *Adv. Funct. Mater.* **2015**, *25*, 3688.
- [25] W. Seung, M. K. Gupta, K. Y. Lee, K. S. Shin, J. H. Lee, T. Y. Kim, S. Kim, J. Lin, J. H. Kim, S. W. Kim, *ACS Nano* **2015**, *9*, 3501.
- [26] Z. Lin, J. Yang, X. Li, Y. Wu, W. Wei, J. Liu, J. Chen, J. Yang, *Adv. Funct. Mater.* **2018**, *28*, 1704112.
- [27] L. Sun, S. Chen, Y. Guo, J. Song, L. Zhang, L. Xiao, Q. Guan, Z. You, *Nano Energy* **2019**, *63*, 103847.
- [28] Y. Li, Y. A. Samad, K. Liao, *J. Mater. Chem. A* **2015**, *3*, 2181.
- [29] C. Wang, K. Xia, M. Jian, H. Wang, M. Zhang, Y. Zhang, *J. Mater. Chem. C* **2017**, *5*, 7604.
- [30] H. Li, Z. Du, *ACS Appl. Mater. Interfaces* **2019**, *11*, 45930.
- [31] M. Zhao, D. Li, J. Huang, D. Wang, A. Mensah, Q. Wei, *J. Mater. Chem. C* **2019**, *7*, 13468.
- [32] R. Paradiso, G. Loriga, N. Taccini, *IEEE Trans. Inf. Technol. Biomed.* **2005**, *9*, 337.
- [33] S. M. Doshi, E. T. Thostenson, *ACS Sensors* **2018**, *3*, 1276.
- [34] D. H. Sung, S. M. Doshi, C. Murray, A. N. Rider, E. T. Thostenson, *Compos. Sci. Technol.* **2020**, *200*, 108415.
- [35] S. M. Doshi, C. Murray, A. Chaudhari, E. T. Thostenson, Proc. IEEE Sensors 2019, October, **2019**, DOI 10.1109/SENSORS43011.2019.8956624.
- [36] B. Mapleback, N. Brack, L. J. Thomson, M. J. S. Spencer, D. A. Osborne, S. M. Doshi, E. T. Thostenson, A. N. Rider, *Langmuir* **2020**, acs.langmuir.0c00018.
- [37] Q. An, A. N. Rider, E. T. Thostenson, *ACS Appl. Mater. Interfaces* **2013**, *5*, 2022.
- [38] C. C. Vu, J. Kim, *Sensors* **2020**, Vol. 20(8), Page 2383
- [39] Y. Li, S. Wang, Z. C. Xiao, Y. Yang, B. W. Deng, B. Yin, K. Ke, M. B. Yang, *J. Mater. Chem. C* **2020**, *8*, 4040.
- [40] P. B. Shull, W. Jirattigalachote, M. A. Hunt, M. R. Cutkosky, S. L. Delp, *Gait Posture* **2014**, *40*, 11.
- [41] Q. An, A. N. Rider, E. T. Thostenson, *Carbon N. Y.* **2012**, *50*, 4130.